

A. JARON\*, Z. ZUREK\*

## NEW POROUS IRON ELECTRODE FOR HYDROGEN EVOLUTION - PRODUCTION AND PROPERTIES

### NOWA POROWATA ELEKTRODA ŻELAZNA DO PRODUKCJI WODORU - OTRZYMYWANIE I WŁAŚCIWOŚCI

A new method of fabrication of porous iron electrode is presented. In due of growing interest for hydrogen production by use of electrochemical technology, the extensively research of new cheaper electrode material currently are lead. At present production of industrial porous metal electrodes is mainly based on fabrication nickel HSE (high surface area) electrodes by sintering of nickel powder in oxygen less atmosphere or etching of Raney alloy to Ni-Raney electrodes.

We proposed to use cheaper porous iron electrodes produced from iron powder instead of the expansive nickel ones. An inexpensive method of production is based on successive oxidation and reduction of the iron powder bed.

This work deals with kinetics of oxidation at 400 and 600°C of iron powder bed in air and water vapor. Thermal effect during oxidation process was determined by DTA/TG analysis. Reduction process of porous oxidized precursor in hydrogen at 600°C was also studied.

The surface morphology of the porous oxidized precursor as well as the received porous metallic iron structure were examined by SEM. The chemical composition was determined by SEM/EDX and XRD analysis.

The optimal condition (i.e. time, temperature) for fabrication process of iron porous electrode with highest specific surface area and open porosity was appointed.

The electrochemical properties of porous iron electrodes (obtained in different conditions of oxidation process) were examined by potentiodynamic measurement. The current-potential dependence was obtained in 1M KOH at 70°C vs. Hg—HgO reference electrode i.e. in conditions corresponding with industrial process of hydrogen production. Hydrogen evolution reaction on iron in conditions mentioned above is considering with the Volmer-Heyrovsky-Tafel kinetic mechanisms. For porous electrode and bulk sample iron and nickel electrodes the  $E^{100}$  potential corresponding for evolution of hydrogen with current density 1000 A/m<sup>2</sup> was determined.  $E^{100}$  potential is assuming values from -1.24 to -1.32 V (depends of sample history) for porous iron electrodes. This potential for bulk iron electrode (-2.96V) and nickel (-1.50V) is significantly higher.

*Keywords:* oxidation, reduction, iron powder

W dobie poszukiwania nowych materiałów o rozwiniętej powierzchni stosowanych w elektrochemicznej produkcji gazów oraz jako nośniki katalizatorów jednym z podstawowych czynników decydujących o ich przydatności jest koszt wytworzenia. Obecnie porowate elektrody przeznaczone do zastosowania w elektrochemii i katalizie przemysłowej otrzymuje się na drodze spiekania proszków metalicznych z podłożem metalicznym lub rozwija się powierzchnię metalu na drodze trawienia np. nikiel Raney'a. W prezentowanym artykule przedstawiano korzystniejszy ekonomicznie sposób wytwarzania porowatych elektrod żelaznych w procesie sekwencyjnego utleniania i redukcji.

W pracy przedstawiono badania kinetyki utleniania proszku żelaza w temperaturze 400 i 600°C w atmosferze powietrza i pary wodnej. Efekty termiczne w czasie procesu utleniania zostały określone na drodze analizy DTA/TG.

Badania procesu redukcji porowatego prekursora tlenkowego prowadzono w temperaturze 600°C w atmosferze wodoru.

Wykonano badania morfologii (SEM) dla otrzymanych spieków tlenkowych jak i porowatych struktur metalicznych otrzymanych w wyniku procesu redukcji. Skład próbek określono przy pomocy analizy SEM/EDX i XRD.

Na podstawie przeprowadzonych badań wyznaczono optymalne warunki (czas, temperatura) procesu wytwarzania porowatej elektrody żelaznej o wysoce rozwiniętej powierzchni właściwej oraz zaproponowano mechanizm utleniania złoża proszku żelaza.

Właściwości elektrochemiczne wytworzonych elektrod oceniono na drodze badań potencjodynamicznych. Zależność prąd-napięcie mierzono w 1M KOH względem elektrody odniesienia Hg—HgO w temperaturze 70°C – w warunkach odpowiadających przemysłowym warunkom otrzymywania wodoru. Mechanizm kinetyki wydzielania wodoru w/w warunkach odpowiada mechanizmowi wg Volmera-Heyrovskiego-Tafela. Dla porowatych elektrod żelaznych oraz próbek żelaznych i niklowych o gładkiej powierzchni wyznaczono potencjał  $E^{100}$  odpowiadający wydzielaniu wodoru prądem o gęstości 1000

\* FACULTY OF CHEMICAL ENGINEERING AND TECHNOLOGY, CRACOW UNIVERSITY OF TECHNOLOGY, UL. WARSZAWSKA 24, 31-155 KRAKOW, POLAND, AJ@CHEMIA.PK.EDU.PL

A/m<sup>2</sup>. Potencjał dla porowatych elektrod żelaznych E100 przyjmował wartości od -1.24 do -1.32 V w zależności od warunków otrzymywania elektrody. Potencjał ten dla elektrody żelaznej (-2.96 V) i elektrody niklowej (-1.50 V) o gładkiej powierzchni jest znacząco wyższy.

## 1. Introduction

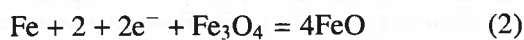
As far as new materials with a developed surface, used in the electrochemical gas production and as catalyst carriers, the production cost is one of the basic factors which decide about their usability. Currently, porous sintered metals intended for use in electrochemistry and industrial catalysis are obtained by process metallic powder sintering with a metallic base, or otherwise, the metal surface is developed through etching, e.g. Raney nickel [1]. The presented paper discusses a more cost-effective method used to manufacture porous sintered iron by thermal-chemical processing of thin powder layers.

## 2. Review of iron oxidation process

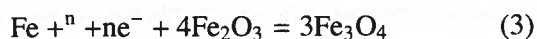
Depending on the temperature and the partial pressure of oxygen in an oxidizing atmosphere, the iron may form one of the three oxides: FeO, Fe<sub>2</sub>O<sub>3</sub> or the mixed Fe<sub>3</sub>O<sub>4</sub> oxide [2]. The mechanism of the three layer oxide on pure iron above 570°C can be described as below [3]. At the iron-wustite interface, the iron ionizes in the following way:



The iron ions and electrons migrate outwards through the FeO layer over the iron vacancies and the electron holes, respectively. At the wustite-magnetite interface, the magnetite is reduced by the iron and the electrons, according to the reaction:

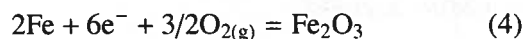


The iron ion and electron surpluses to this reaction proceed outward through the magnetite layer, over the iron vacancies on the tetrahedral and octahedral sites and over the electron holes and the excess electrons, respectively. At the magnetite-haematite interface, the magnetite is formed according to reaction:

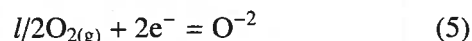


where the value of n is two and three, for the Fe<sup>+2</sup> and Fe<sup>+3</sup> ions, respectively.

If the iron ions are mobile in the haematite, they will migrate through this phase over the iron ion vacancies  $V_{\text{Fe}}$  together with the electrons, and a new haematite will form at the Fe<sub>2</sub>O<sub>3</sub>-gas interface, according to reaction:



At this interface, the oxygen also ionises according to the reaction:



If the oxygen ions are mobile in the haematite layer, the iron ions and electrons which are in excess of the number required for the reduction of the haematite to a magnetite, will react with the oxygen ions, diffusing inwards through the Fe<sub>2</sub>O<sub>3</sub> layer over the oxygen vacancies, forming a new Fe<sub>2</sub>O<sub>3</sub>, according to the reaction:



The corresponding electrons then migrate outward through Fe<sub>2</sub>O<sub>3</sub> to take part in the ionisation of oxygen at the Fe<sub>2</sub>O<sub>3</sub>-gas interface.

Since the scale formed at temperatures above 570°C is predominantly FeO, the growth of this layer controls the overall oxidation kinetics. Due to the rapid reaction rates, the scale adhesion is lost, in spite of the relatively high plasticity of FeO. This results in the formation of a highly porous inner layer of FeO.

It means that, under 570°C, the forming scale consists of Fe<sub>3</sub>O<sub>4</sub> / Fe<sub>2</sub>O<sub>3</sub>, whereas at higher temperatures, the scale would contain all three oxides in sequence – FeO, Fe<sub>3</sub>O<sub>4</sub>, Fe<sub>2</sub>O<sub>3</sub> [4]. The scale grows due to the outward iron cation diffusion and the inward oxygen diffusion [5].

In the case of the Fe-C system in the 400 – 600°C temperature range, the carbonization process does not proceed – the carbon is only oxidized to oxides. This was confirmed by a computer simulation (FastSage 5.3.1 [6]) using the Gibbs potential minimization method. The calculations were performed for the {3 mol Fe + 1mol C + synthetic air} system, on the assumption of an oxidant surplus. On the condition mentioned above, the hematite will be the main solid phase and CO<sub>2</sub> will be the main gas phase.

In the case when steam is used as the oxidant, the following mechanisms are suggested: a rapid oxidant transport to the scale/metal interface [7], diffusion [8], and a formation of bridges H<sub>2</sub>/H<sub>2</sub>O [9]. Previous tests [10] and the studies carried out at Forschungszentrum Jülich [11] provided grounds to determine that the iron oxidation in the steam takes place as a result of an unstable iron hydroxide formation. This process has been

proposed by Surman [12,13], and it assumes that the iron oxidation rate is dependent on the evaporation process of  $\text{Fe}(\text{OH})_2$ , which is formed at the metal/oxide phase boundary and decomposes to  $\text{Fe}_3\text{O}_4$  at the scale/gas phase boundary.

### 3. Materials and test procedures

The iron powder Fe DAB 7 (from Merck), purity 99.99, was selected as the test material. A narrow grain distribution (the whole fraction  $< 20 \mu\text{m}$ ) is characteristic for this powder; an average grain diameter is  $10 \mu\text{m}$ . Powder samples in 0.25mm-thick iron foil containers ( $10\text{mm} \times 10\text{mm} \times 0.5\text{mm}$ ) were prepared in order to carry out the oxidation and then – the reduction experiments. A mixture of 3 mol Fe : 1 mol C powders was also used. The used carbon powder was wood coal purity 99.9 and the grain diameter was from 5 to  $20 \mu\text{m}$ . The

oxidation process was carried out both in dry synthetic air at the flow rate of  $10 \text{dm}^3/\text{h}$ , and in steam atmosphere with an argon addition. The steam and the argon flow rate was  $350 \text{dm}^3/\text{h}$  and  $5 \text{dm}^3/\text{h}$ , respectively. The tests were performed at 400 and  $600^\circ\text{C}$ . The reduction process was carried out in hydrogen at the atmospheric pressure and at the temperature of  $600^\circ\text{C}$ .

The oxidation and reduction kinetics was tested for the Fe DAB 7 powder layers (thickness 1mm,  $\phi$  9mm) in order to determine the duration of the oxidation and the reduction experiments. The tests were performed with a standard thermogravimetric equipment, including computer measurement recording. The obtained results (Fig.1) allowed to determine that the time of the oxidation experiments using the discontinuous method ranged from 10 to 100 minutes, and the time of the reduction with hydrogen was 2 hrs. An untypical oxidation kinetics dependence (a higher weight gain at a lower temperature) is discussed in [14].

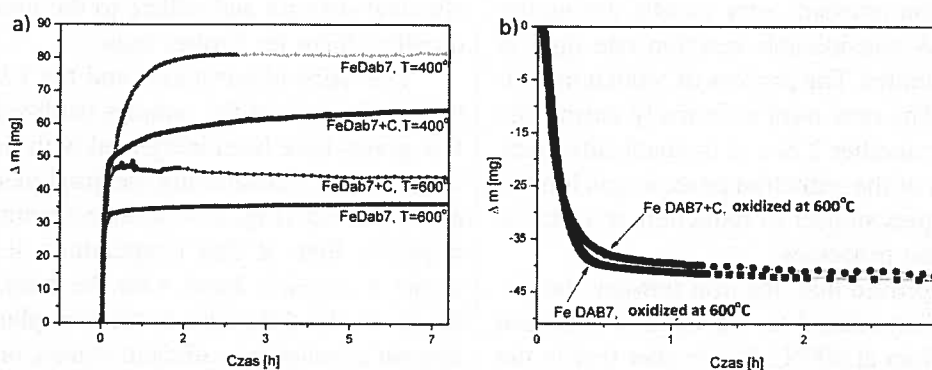


Fig. 1. (a) Kinetics of oxidation processes of Fe DAB 7 and Fe DAB 7 + C powders at 400 and  $600^\circ\text{C}$  in air; (b) kinetics of reduction processes of Fe DAB 7 and Fe DAB 7 + C powders oxidized at  $600^\circ\text{C}$  in air

The oxidation and reduction experiments were carried out in tubular furnaces with a loop water seal, equipped with electronic temperature controllers (accuracy  $\pm 5^\circ$ ). The experiment system was each time washed for 15 minutes with argon at room temperature, and the warming-up was carried out in argon atmosphere. This was done in order to eliminate the effects related to the varying warm-up time, depending on the preset temperature.

The DTA tests (standard apparatus: Universal V2.3C TA Instruments) were performed for the Fe DAB 7 and Fe DAB 7 + C powders, in order to eliminate the effect of powder deposit overheating during the oxidation. During the DTA experiments, thin layers of the powder sample and the reference substance ( $\text{Al}_2\text{O}_3$ ) were placed in an identical relation to the thermal capacity of the ceramic crushables (inert in the test condition). The system was brought to the preset temperature in inert gas atmosphere

(Ar), and kept at that temperature for 15 min. Then the synthetic air was let into the system. Each time after letting in the air, a  $10^\circ\text{C}$  temperature increase was observed in the measurement chamber due to the different thermal capacities of argon and air. Moreover, an exoenergetic effect was recorded (each time – a single peak) with a simultaneous sample weight growth, which allowed to link it with the powder deposit oxidation. The values of the exoenergetic effect at the temperature of  $400^\circ\text{C}$  for the Fe DAB7 powder and the Fe DAB7 + C powder, were  $1.5680^\circ\text{C}\cdot\text{min}/\text{mg}$  and  $0.7703^\circ\text{C}\cdot\text{min}/\text{mg}$ , respectively; at the temperature of  $600^\circ\text{C}$  –  $0.3494^\circ\text{C}\cdot\text{min}/\text{mg}$  for the Fe DAB7 powder and  $1.2270^\circ\text{C}\cdot\text{min}/\text{mg}$  for the Fe DAB7 + C powder. However, the value of this effect is too small to cause a considerable powder layer overheating on the iron base (in the container).

The potentiodynamic tests were performed using a potentiostat-galvanostat (ATLAS 9833) controlled by

the POL-99 application. The current-voltage relation for the tested electrodes was obtained by potential scanning within the range from -1V to -1.35 V, with a 0.025 V / 10 min step, relative to the reference electrode Hg/HgO. Samples of powder electrodes and iron foil (purity 99.9%) were used in the tests. The long duration of each step was assumed to achieve the brief state of equilibrium during the hydrogen evolution. The area of the samples was limited to 1 cm<sup>2</sup>, which was achieved by submerging them in epidian resin. Additionally, the iron foil electrodes were polished by Al<sub>2</sub>O<sub>3</sub> powder (to 0.3-*mu*pm grain). The electrochemical measurements were carried out in a 1 M KOH solution, at the temperature of 70°C.

#### 4. Results and discussion

The kinetics shown in Fig. 1a indicates that, independently of the powder deposit's temperature and composition, the oxidation proceeds very rapidly during the first process stage. A considerable reaction rate drop is observed after 30 minutes. The process of reduction with the hydrogen (Fig. 1b) runs most effectively during the first 2 hrs, and after another 2 hrs, it is practically completed. The duration of the reduction process was limited to 2 hrs, in the samples subject to reduction, in order to avoid recrystallization processes.

The DTA tests proved that, for iron powder, the deposit exothermic effect related to the deposit oxidation is higher at 400°C than at 600°C. Remember that in the case of the powder deposit, we deal with two processes: grain oxidation and oxide layer formation on the powder

deposit surface – a higher exothermic effect obtained at a lower temperature proves a better oxidant access to the deposit inside, due to a slower formation of the oxide barrier on the deposit surface. This result is consistent with the results of the research on the oxidation kinetics, and it has been confirmed by sample fracture observation carried out with an electron microscope. A reversed thermal effect relation for samples with a carbon addition proves that the oxidation process proceeds more rapidly at 600°C. The oxidation is in most part related to the carbon oxidation, which is not identified in the samples analysed after the oxidation process (SEM+EDX, XRD).

The sinter mechanical stability assessment brings to the conclusion that, in the case of the samples oxidized at 400°C, we deal with a lack of mechanical stability in the powder layer, which is not permanently bound with the metallic base (independently of the powder composition and the oxidizing atmosphere). A high brittleness was characteristic for sinter without a base.

The samples oxidized at 600°C possess a good mechanical strength and adhere to the metallic base, which qualifies them for further tests.

The SEM observations and the EDX analysis show that, in the case of the samples oxidized at 400°C, only a few grains have been integrated with the base by oxidizing (Fig. 2a). Considering the good oxidant access to the deposit inside (Fig. 2b – sample fracture, high porosity), it proves that, at this temperature, it is impossible to create a cohesive bond with the base. This effect may be due to the difference in the iron plate and the powder deposit expansion coefficient values, or the observed deposit shrinkage during the oxidation – sintering at that temperature.

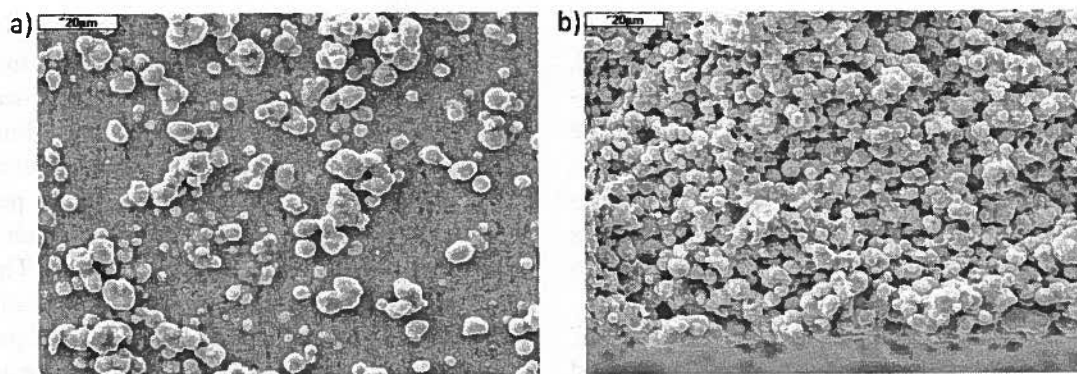


Fig. 2. Sample oxidized at 400°C, 70 min, air: (a) cohesive bonded grains on the base, (b) fracture (next to the base)


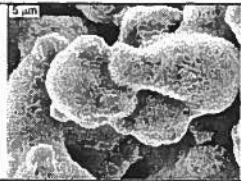
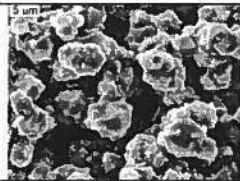
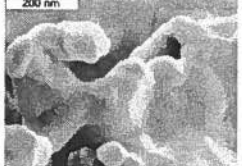
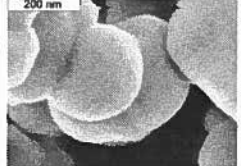
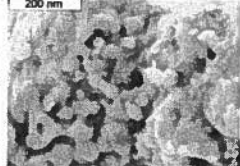
The SEM observations of the samples subject to oxidizing at 600°C allowed to determine the oxidation time, after which the layers on the metallic base (depending on the composition and the applied oxidant) show a maximum grain surface development and open porosity.

The time for the Fe DAB 7 powder samples oxidized in air is 30 min., and for the samples oxidized in steam atmosphere, it is 40 min. For the Fe DAB 7 + C powder samples in air atmosphere, the time is 20 min.

The results of the SEM observations for the samples obtained in the conditions specified beforehand and after the reduction with hydrogen are shown in Tab. 1. Characteristic for the samples oxidized in air were larger

grains, each strongly overgrown, with a developed surface. This structure was maintained after the reduction in hydrogen.

TABLE 2  
Microphotographs of iron powder sinters obtained by oxidation at 600°C before and after reduction processes.

Sample composition / atmosphere / time	Fe DAB 7 / air / 30 min	Fe DAB 7 + C / air / 20 min	Fe DAB 7 / H <sub>2</sub> O vapour / 40 min
Oxidized surface (before reduction)			
Surface after reduction in H <sub>2</sub> (600°C, 2h)			

The samples with a carbon addition show smaller grains with a maintained “neck” in the grain contact areas. The grains show a very strongly developed surface, which, after the reduction, forms an individual texture on the grain surfaces. The reduction process causes the “etching” of the necks in the inter-grain contact areas, which leads to a formation of high open porosity.

The grains of the samples subject to oxidizing in steam atmosphere show the lowest surface growth during the oxidation. The process of oxidation in steam leads to a transformation of the spherical powder grains into acute angle irregular polyhedrons. Due to the reduction of thus obtained sinter, we receive a very finely grained

structure with many small pores. The grains maintain their irregular shape formed as a result of the oxidation process.

The electrochemical investigations were carried out on the samples prepared in the way described above. After 12 hours of the electrode's work, no essential changes in the electrode surface morphology are observed during the electrolytic hydrogen release from 1M of the KOH solution at the temperature of 70°C. The formed small blooms (visible in Fig. 3) consist of potassium and oxygen (the EDX analysis); however the amount of these elements on the sample surface is less than 5%<sub>at</sub>.

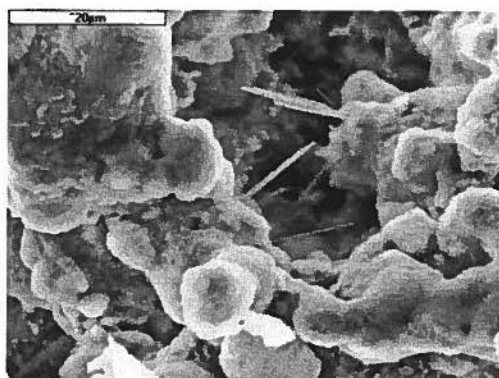


Fig. 3. Microphotography of iron porous electrode surface (oxidation: 30min, 600°C, air, reduction: 2h, 600°C) after 12h of work in 1M KOH, 70°. EDX analysis from showed area: Fe – 87.9%<sub>at</sub>, K – 4.9%<sub>at</sub>, O – 2.3%<sub>at</sub>, rest – 4.9%<sub>at</sub>

The electrodes obtained by oxidation in 10 and 100 minutes, and 30 min (air), 20 min (Fe+C) and 40 min (steam), were subject to potentiodynamic tests during the process of the cathodic hydrogen evolution. The current-voltage characteristics were determined for the tested electrodes (Fig. 4). The measurements were carried out in 1 M KOH at the temperature of 70°C, which corresponded to the conditions applied during the electrolytic hydrogen generation in industrial processes.

Three zones may be distinguished on all the curves. The first zone, from -1.000 to -1.050 V, is related to the reduction of the oxides generated after the submerging of the iron electrode in a hot hydroxide solution. The process of a slow hydrogen evolution on the electrode takes place in the zone between -1.050 to -1.250 V. Under -1.250 V, we observe a semi-linear area related to the rapid hydrogen evolution on the porous iron electrodes.

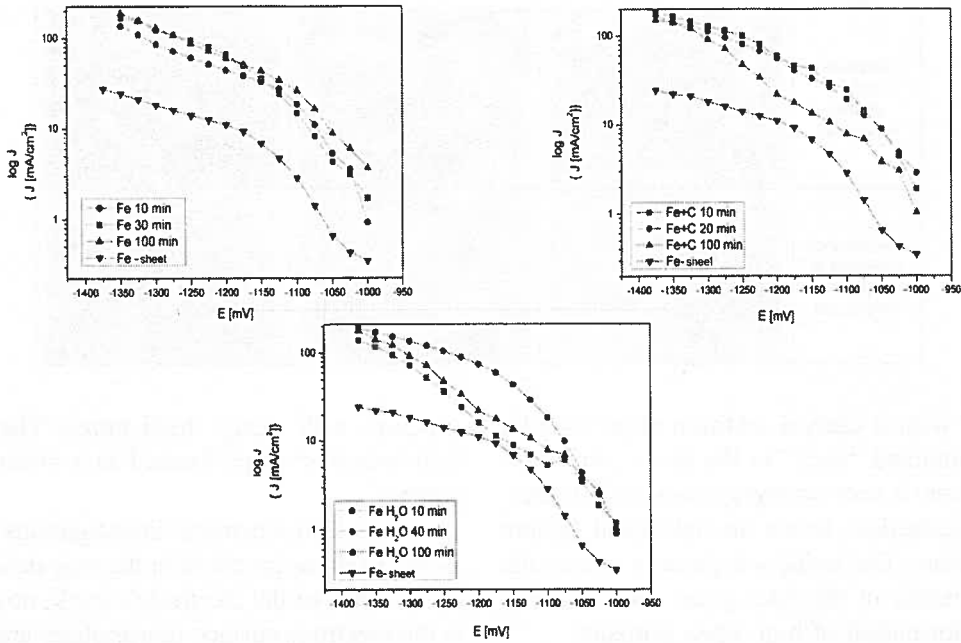


Fig. 4. Current-potential dependence (vs. Hg/HgO) for iron porous electrodes obtained by way of oxidation/reduction and Fe sheet

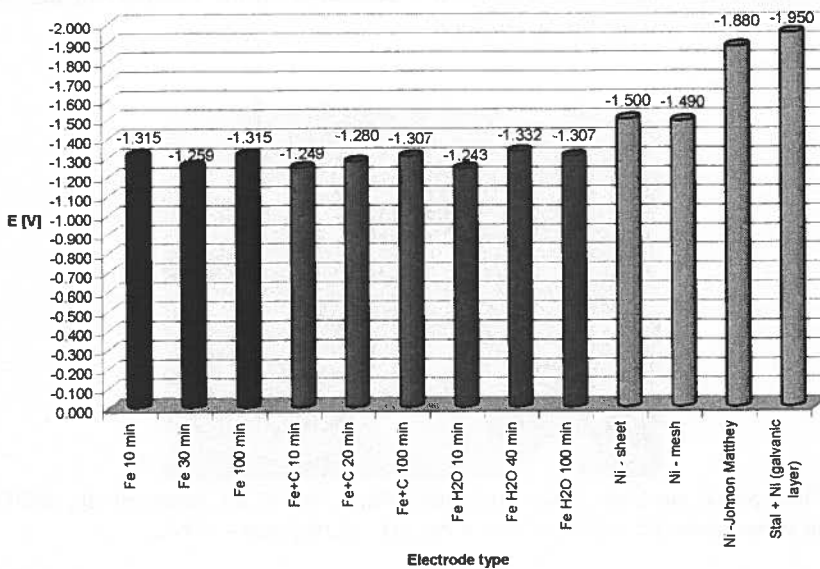


Fig. 5. E<sup>100</sup> potentials values for nickel and iron electrodes

The porous iron electrodes have much lower hydrogen evolution voltage values, as compared to the solid iron electrode (Fig. 4), and to the nickel electrodes (plate and mesh – 99.9% Ni).

The diagram (Fig. 5) shows compiled potential  $E^{100}$  values, corresponding to the hydrogen evolution with the current of a  $1000 \text{ A/m}^2$  density for the porous iron electrodes, the solid iron and the nickel electrodes. According to the compiled data, the lowest value of  $E^{100} = -1.243 \text{ V}$  is given for the electrode obtained by oxidation in 10 minutes in steam, which fully correlates with the results of the observations involving electrode surface development (SEM).

### 5. Conclusions

Iron powder oxidation at the temperature of  $600^\circ\text{C}$  allows to form porous oxide structures with a developed surface and good mechanical properties.

The morphology of the obtained structures may be controlled via the powder composition or the oxidizing atmosphere composition.

The process of reduction by hydrogen at the temperature of  $600^\circ\text{C}$  allows to form porous iron electrodes with a developed surface.

The surface of the porous iron electrodes was stable during the electrochemical test in an alkaline solution.

The lowest value of  $E^{100} = -1.243 \text{ V}$ , obtained during the process of the electrolytic hydrogen evolution in industrial conditions, was determined for the electrode obtained by oxidation in 10 minutes ( $600^\circ\text{C}$ ) and the reduction with hydrogen at 2h,  $600^\circ\text{C}$ . An application of the same oxidation and reduction temperature allows to carry out the electrode production process sequentially, using one apparatus and skipping the cooling down stage.

Characteristic of the oxide sinters obtained at the temperature of  $400^\circ\text{C}$  is a high brittleness, which makes it impossible to use them in porous iron electrode production processes.

### REFERENCES

- [1] A. Kowal, *Chemia Stosowana*, XXXIV, 3-4, 157-176 (1990).
- [2] A. Bielanski, *Chemia ogólna i nieorganiczna*, Wydanie VII, PWN, Warszawa, 589 (1981).
- [3] A. S. Khanna, *Introduction to High Temperature Oxidation and Corrosion*, ASM International, 85 (2002).
- [4] S. Mrowec, T. Werber, *Korozja Gazowa Metali*, Wydawnictwo Śląsk Katowice, 207 (1965).
- [5] N. Birks, G. H. Meier, *Introduction to High Temperature Oxidation of Metals*, 74 (1982).
- [6] Program: FactSage 5.3.1 – Integrated Thermodynamic Databank System, Thermafact 1976-2004.
- [7] A. Galerie, Y. Wouters, M. Caillet, *Mat. Sci. Forum* **369-372**, 231 (2001).
- [8] Y. Ikeda, K. Nii, *Transactions of Nat. Res. Inst. for Met.* **26**, 1, 52 (1994).
- [9] A. Rahmel, J. Tobolski, *Corros. Sci.* **5**, 333 (1965).
- [10] A. Jaron, Z. Zurek, A. Stawiarski, J. Zurek, M. Homa, *Ochr. przed kor.*, 11s/A/2003, 97-101 (2003).
- [11] R. Michalik, *Water vapour influence on the oxidation mechanism of ferritic Cr-steels.*, Thesis, Jülich 23-32 (2002).
- [12] P. L. Surman and J. E. Castle, *Corros. Sci.*, vol. 9, (1969), 771.
- [13] P. L. Surman, *Corr. Sci.*, vol. 13, 113 (1973).
- [14] A. Jaron, Z. Zurek, T. Werber, *Ochr. przed kor.*, 11s/A/2004, 39-42, (2004).